Chapter 2

Numerical models

2.1 Introduction

In general terms the objectives of the thesis have been the development of infrastructure and the elaboration of methodology, permitting the generation of experimental data and the validation of numerical models in the fields of refrigeration and air conditioning. At the present stage, the work has been orientated to the creation of means for experimental validation of two mathematical models: a numerical model of liquid overfeed refrigeration systems, and a model of compact heat exchangers, presented subsequently. These models have been important in the developing phase to assist the design process of the experimental infrastructure, for parametric studies determining the working range, selection of the equipment, prototypes' definition and instrumentation.

The formulation of the liquid overfeed refrigeration system model presented first in [1], is exposed in detail here. The model is based on sequential resolution of the different elements of the system (compressor, condenser, evaporator, etc.). For each element global balances of mass, momentum and energy are applied. The model can determine the operating point of the system in basis of either internal parameters (evaporating and condensing temperatures), or external parameters as the inlet temperatures and flow-rates of the secondary fluids in the evaporator and the condenser. The heat losses or gains and the pressure losses in the tubes connecting the elements of the system are calculated. The model gives as an output the temperatures, pressures, mass and volumetric flow-rates in all significant points of the system. The refrigerant velocities in the tubes are also calculated in order to check if they are within the limits prescribed from the engineering practice. Considering the characteristics of the model, it can be used as a tool for system optimization, analysis and design.

Description of the numerical model for simulation of compact heat exchangers is also presented. The model has been developed in CTTC, undergoing numerous improvements in the last years, and subject of various publications [2], [3]. It has been consoli-

dated under the name CHESS (Compact Heat Exchangers Simulation Softwear). The model adopts a strategy of resolution based on discretization of the heat exchanger into macro control volumes around the tubes. Over these macro control volumes the equations for conservation of mass, momentum and energy are applied for both fluids, and the energy equation is applied for the tubes and fins. The model permits different levels of detail in the simulation of the flow inside the tubes, the air-flow, and the solid elements, compromising between accuracy and required computational time for resolution.

2.2 Liquid overfeed refrigeration system model

The model has been developed as a system analysis and design optimization tool, [1]. The global algorithm is based on the sequential resolution of the different elements of the system, for each of which a simplified mathematical model is used. The elements of the system are modelized on a basis of global balances of mass, momentum and energy, using information from higher level simulations for the heat transfer coefficient and the pressure loss in the evaporator, and manufacturer data for characterizing the compressor, the brazed plate condenser and the auxiliary heat exchanger. The pressure losses and the heat losses or gains in the connecting tubes of the system are calculated. Correlations for the single- and two-phase friction factor, and empirical information for the local pressure loss in singularities are used. The overall heat transfer coefficient in the tubes is calculated on the basis of the inner heat transfer coefficient (single- or two-phase), the heat conduction properties of the tubes and the insulation, and the outside heat transfer coefficient.
The model gives as an output the evaporating and condensing capacities, and the temperatures, pressures and flow-rates throughout the system.

2.2.1 Description of the liquid overfeed system

Liquid overfeed refrigeration systems are those in which to the evaporator is delivered a greater rate of liquid refrigerant than the evaporated. At the exit of the evaporator a mixture of liquid and vapour flows out. These systems are characterized for having a low-pressure receiver from which the liquid refrigerant is circulated through the evaporator either mechanically or using gas pressure. The liquid-vapour mixture from the evaporator is returned to low-pressure receiver. The vapour is directed to the compressor. The refrigerant enters the low-pressure receiver by means of metering device, usually maintaining constant refrigerant level. A scheme of the refrigeration system with mechanical liquid overfeed of the evaporator is shown in Figure 2.1. The system has two principal circuits, one passing through the compressor (points 1 to 14), and another passing through the evaporator (points 101 to 107), having different

flow-rates. When halocarbon refrigerants miscible with oil are used, although using highly efficient oil separators after the compressor, an appropriate system for oil management is necessary. A third circuit (between points 201 and 204) is usually used for oil recuperation from the low pressure side of the installation. A small quantity of refrigerant is drawn through this circuit and completely evaporated in an auxiliary heat exchanger. The refrigerant vapour and the contained oil are returned to the compressor introducing them into the suction line at point 204, assuring the proper functioning of the compressor.
The principal advantages of the liquid overfeed systems are high efficiency and reduced operating expenses. These systems have lower energy costs, operate less hours to produce the same cooling capacity, and need less maintenance than direct expansion systems because of several advantages, [4], the most important of which are:

- The evaporator surface is used efficiently through good refrigerant distribution and completely wetted internal tube surfaces.
- The compressors are protected. Liquid slugs resulting from fluctuating loads or malfunctioning controls are separated from suction gas in the low-pressure receiver.
- Low suction super-heats are achieved where the suction lines between the low-pressure receiver and the compressors are short. This causes lower discharge temperatures, preventing lubrication breakdown and minimizing condenser fouling.
- Refrigerant feed to evaporators is unaffected by fluctuating ambient condensing conditions.
- Flash gas resulting from refrigerant throttling losses is removed at the low-pressure receiver before entering the evaporators. This gas is drawn directly to the compressors and eliminated as a factor in the design of the system low side.
- Because of ideal entering suction gas conditions, compressors last longer. There is less maintenance and fewer breakdowns. The oil circulation rate to the evaporators is reduced as a result of the low compressor discharge super-heat and separation at the low-pressure receiver.
- Overfeed systems have convenient automatic operation.

There are some possible disadvantages of the liquid overfeed systems:

- In some cases, refrigerant charges are greater than those used in other systems.
- Higher refrigerant flow rates to and from evaporators cause the liquid feed and wet return lines to be larger in diameter than the high-pressure liquid and suction lines for other systems.
- Piping insulation, which is costly, is generally required in all feed and return lines to prevent condensation, frost formation and heat gain.
- The installed cost may be greater, particularly for small systems or those having fewer than three evaporators.
- The pumping units may require maintenance.
- Pumps sometimes have cavitation problems due to low available net positive suction pressure.

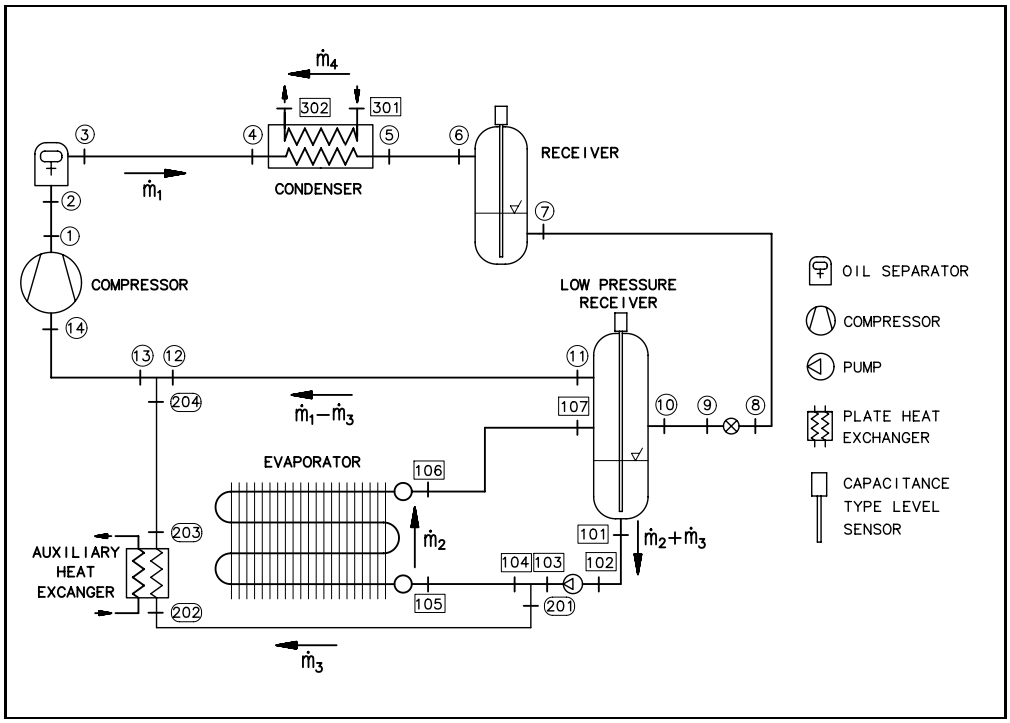

Figure 2.1: Liquid Overfeed Refrigeration Facility Scheme

The advantages of liquid overfeed systems become dominant in low temperature installations and where there exist multiple evaporators, [5]. In low temperature applications achieving good heat transfer in evaporators is crucial for the system efficiency. The plants operate with high compression ratios and appreciable quantities of flash gas, and the high suction super-heat could be a problem. When the number of evaporators is small, flooded evaporators can be applied with the same effectiveness as liquid overfeed evaporators. Since oil return provisions must be made for each coil in systems with flooded evaporators, when the number of coils exceeds 3 to 5, it is usually more beneficial to choose liquid overfeed system where the oil is removed at only one point: the low-pressure receiver.
Liquid overfeed systems may have advantages also in higher temperature systems used for air conditioning, where improved heat transfer coefficients and positive feeding of multiple evaporators may be achieved. When halocarbon refrigerants miscible with oil are used, oil is conveyed to the low-pressure side, and a central oil return can be provided in the low-pressure receiver, rather than running the risk of oil accumulation in some evaporators, existent with direct expansion systems.

2.2.2 Numerical simulation

A numerical simulation of a liquid overfeed system working with pure refrigerants in steady state conditions is developed. The algorithm is based on sequential resolution of the different elements of the system, which are modelized on the basis empirical parameters from higher level simulations, manufacturer data, and global balances of mass, momentum and energy. The thermo-physical properties of the refrigerant throughout the system are evaluated with REFPROP, [6]. The structure of the simulation program is shown schematically in Figure 2.2.

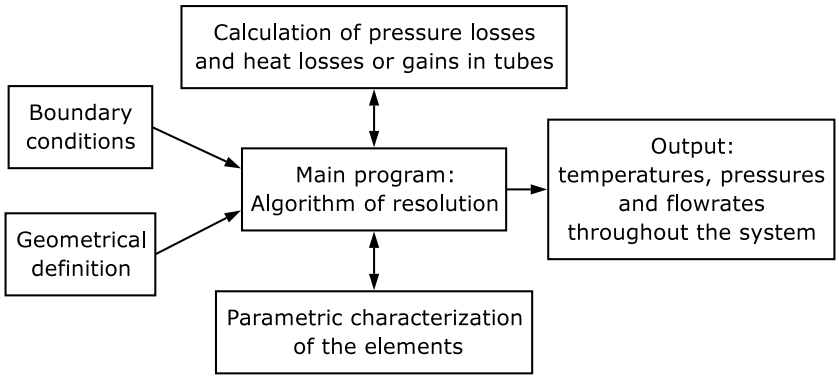

Figure 2.2: Simulation program structure

The program predicts the operating point of the system, calculating the temperatures, the pressures, and the refrigerant flow-rates throughout the system, under the defined boundary conditions, geometry and the equipment characteristics. The program is structured in several blocks feeding with the necessary information the main program, which is encharged to perform the resolution algorithm.

The boundary conditions for calculation can be given on a basis of either external parameters, as the inlet temperatures and flow-rates of the secondary fluids in the evaporator (air) and the condenser (water), or on a basis of internal parameters, as evaporating and condensing temperatures. This can be decided depending on the objectives aimed with the simulation. The circulating rate of the refrigerant is given as an input. This permits fast parametric analysis in this important aspect, and evaluation of its impact over the whole system performance, with the subsequent considerations in designing the system. The sensible heat ratio (SHR) should be also defined in order to calculate the air temperature at the outlet of the evaporator.

The geometry of the refrigeration system is defined in a separate block. The tubes connecting two elements of the system represent a single tube section, for which the length, the tube size, insulation thickness and type, and number and type of singularities producing local pressure losses (valves, elbows, etc.), are defined. The height difference between inlet and outlet of the tube section is considered through a hypothetical inclination angle and the whole length. For each tube section a different ambient temperature can be defined in order to calculate the heat losses or gains in each section, taking into account that some of the tubes are exposed to the ambient, and other are within the cold room.

Another block in the simulation program is dedicated to the parametric characterization of the different elements of the system. The characterization includes the data for the global heat transfer and the flow configuration factor in the evaporator, the condenser and the auxiliary heat exchanger. The compressor has been characterized using data from the manufacturer about the power consumption, refrigerant flow-rate and efficiency.

The pressure losses in the connecting tubes of the system are calculated, evaluating the pressure losses due to friction, local pressure losses and difference of height between inlet and outlet. The friction factor is calculated from empirical correlations considering single and two-phase flow [7], [8], [9]. The heat losses or gains in the connecting tubes are also calculated, using a global heat transfer coefficient considering the inner and outer heat transfer coefficients and the thermal resistances in the tube and the insulation. For the inner heat transfer coefficient correlations for single and two-phase flow have been used [10], [11]. For the outer heat transfer coefficient natural convection around the tubes is considered.

2.2.3 Mathematical equations for modelling of the elements

The present numerical model has been developed for steady state conditions and pure refrigerant fluids. The different elements of the system are resolved applying over them the necessary conservation principles of mass, momentum and energy. The three circuits indicated in Figure 2.1 are: i) compressor circuit (point 1 to 14); ii) evaporator circuit (points 101 to 107); iii) auxiliary circuit for oil return (points 201 to 204). In this section, the equations used in these balances are presented for each element of the system.

Evaporator. A set of equations representing the global heat exchanged in the evaporator is obtained. The mass flux through the evaporator, the evaporator capacity and the outlet temperature of the secondary fluid are calculated from the following equations:

$$\dot{Q}_e = \dot{m}_2(h_{106} - h_{105}) \tag{2.1}$$

$$\dot{Q}_e = \dot{m}_a c_{p_a}(T_{a,i} - T_{a,o}) \tag{2.2}$$

$$\dot{Q}_e = U_{o,e} F_e A_{o,e} \Delta T_{lm,e} \tag{2.3}$$

$$h_{106} = f(p_e, x_{g106}) \tag{2.4}$$

where the inlet temperature $T_{a,i}$ and the mass flux $\dot{m}_a$ of the air are known as boundary conditions. The circulating rate is given as an input, and the outlet vapour quality is calculated from it, assuming saturation conditions at the inlet section of the evaporator, x_{g106}=1/[circulating rate]. The global heat transfer coefficient and the flow configuration, $U_{o,e}F_e$ are computed with the advanced numerical simulation developed for fin-and-tube heat exchangers, and have been correlated in function of $\Delta T_{lm,e}$, circulating rate and air velocity. The pressure drop through the evaporator is evaluated from a correlation created in function of the circulating rate and the cooling capacity, calculated from advanced numerical simulation. For the evaluation of the physical properties REFPROP [6] is used.

Condenser. A set of equations representing the heat transfer in the condenser is obtained. The refrigerant outlet enthalpy, the outlet temperature of the secondary fluid, and the condenser capacity are calculated from the following equations:

$$\dot{Q}_{cd} = \dot{m}_1(h_5 - h_4) \tag{2.5}$$

$$\dot{Q}_{cd} = \dot{m}_{cd,s} c_{p_{cd,s}}(T_{cd,si} - T_{cd,so}) \tag{2.6}$$

$$\dot{Q}_{cd} = U_{o,cd} F_{cd} A_{o,cd} \Delta T_{lm,cd} \tag{2.7}$$

$$h_5 = f(p_5, T_5) \tag{2.8}$$

The product of the global heat transfer coefficient, the flow configuration factor $U_{o,cd}F_{cd}$ and the refrigerant pressure loss are parametrised from manufacturer's data

in basis of the refrigerant and secondary fluid flows, as it is done for the evaporator. The inlet temperature $T_{cd,si}$ and the mass flux $\dot{m}_{cd,s}$ of the secondary fluid are known as boundary conditions.

Compressor. The compressor is characterized from manufacturer data through the electrical power consumption ($\dot{W}_E$), the electrical-mechanical efficiency (η_{em}) and the refrigerant mass flow ($\dot{m}_1$) as functions of the refrigerant fluid, suction and discharge pressures, and the suction vapour super-heat of the refrigerant. For the selected compressor and refrigerant fluid, matrices with values of the electrical power and the mass flow in the working range are generated. When a value between the calculated matrix points is required, it can be obtained by interpolation between the nearest 4 points.

The mechanical power applied to the fluid in the compressor ($\dot{W}_{cp}$) and the discharge enthalpy (h_1) and temperature (T_1) are obtained from the equations:

$$\dot{W}_{cp} = \dot{W}_E \eta_{em} \tag{2.9}$$

$$\dot{W}_{cp} = \dot{m}_1 (h_1 - h_{14}) \tag{2.10}$$

$$h_1 = f(p_1, T_1) \tag{2.11}$$

Expansion device. The expansion mechanism is considered adiabatic (h_9=h_8).

Pump. The pumping power applied to the fluid is obtained from the pressure losses in the pump circuit (liquid refrigerant feed tubes, evaporator and wet return tubes) and the volumetric flow-rate, equation (2.12). From the energy balance, equation 2.13, the outlet enthalpy (h_{103}) is determined.

$$\dot{W}_p = \Delta p_p (\dot{m}_2 + \dot{m}_3)/\rho \tag{2.12}$$

$$\dot{W}_p = (\dot{m}_2 + \dot{m}_3)(h_{103} - h_{102}) \tag{2.13}$$

Receiver. If the receiver is considered adiabatic, the outlet condition in this element corresponds to saturated liquid at its corresponding pressure due to the system working conditions, because this element is designed to contain always a liquid and vapour refrigerant phases.

Low-pressure receiver. In this element, with two inlets and two outlets, the conditions of points h_{101} and h_{11} are saturated liquid and saturated vapour at the pressure of the low-pressure receiver. With this information and from an energy balance, the enthalpy h_{101} or the enthalpy h_{11} is obtained, and from this, the pressure in the low-pressure receiver is calculated.

$$\dot{m}_1 h_{10} + \dot{m}_2 h_{107} + \dot{Q}_{lpr} = (\dot{m}_2 + \dot{m}_3) h_{101} + (\dot{m}_1 - \dot{m}_3) h_{11} \tag{2.14}$$

$$h_{101} = h_{l,sat}(p_{101}) \tag{2.15}$$

Tubes. For each section between two points in the Figure 2.1, that only includes tubes and singularities (valves, elbows, contractions, expansions, etc.), the heat loss or gain and the pressure loss are calculated from the following equations:

$$U_i A_i \Delta T_{lm} = \dot{m} \left(h_{out} - h_{in} \right) \tag{2.16}$$

$$\left(p_{out} - p_{in} \right) S - \Delta p_{fr} A - \Delta p_{loc} A - mg\Delta z = \dot{m} \left(v_{out} - v_{in} \right) \tag{2.17}$$

The pressure loss in each section is due to flow friction Δp_{fr} and local pressure loss through singularities Δp_{loc}:

$$\Delta p_{fr} = f \frac{\rho v^2}{2} \tag{2.18}$$

$$\Delta p_{loc} = k \frac{\rho v^2}{2} \tag{2.19}$$

Empirical correlations for the calculation of the friction factor (f) inside the tubes have been used, considering single or two-phase flow [7], [8] or [9]. For the local pressure loss factor (k) through the singularities empirical coefficients from [12] have been used.
The pressure changes due to height difference (Δz) between the inlet and outlet of the tube section are considered in the equation (2.17) with the term $mg\Delta z$.
For the calculation of the heat fluxes in the tubes, the global heat transfer coefficient for each section is calculated considering the inner and outer heat transfer coefficients (α_i and α_o) and the thermal resistances of the tube and the insulation.

$$U_i = \left[\frac{1}{\alpha_i} + \frac{D_i}{2\lambda_{ins}} \ln \left(\frac{D_{ext}}{D_o} \right) + \frac{D_i}{2\lambda_{tube}} \ln \left(\frac{D_o}{D_i} \right) + \frac{D_i}{D_o \alpha_o} \right]^{-1} \tag{2.20}$$

For the computing of the inner heat transfer coefficient α_i, correlations for single and two-phase flow have been used [10], [11]. For the outer coefficient α_o, natural convection around tubes has been considered.
Calculation of additional mass fluxes. In the case of halocarbons, the mass flux $\dot{m}_3$ is calculated supposing that the whole quantity of oil after the oil separator is returned to the compressor from the auxiliary circuit, preventing in this way malfunctioning of the compressor. The oil concentration in the refrigerant after the oil separator (M_{sep}) [kg oil/kg ref] is data given by the oil separator characteristics, and the concentration of oil in the low-pressure receiver (M_{lpr}) [kg oil/kg ref] is an input establishing the working conditions of the system. The flow-rate needed to be extracted from the low-pressure receiver, completely evaporated and returned to the compressor in order to maintain the imposed quantity of oil in the low-pressure side is:

$$\dot{m}_3 = \frac{M_{sep}}{M_{lpr}} \dot{m}_1 \tag{2.21}$$

Auxiliary heat exchanger. A set of equations representing the heat exchange in the auxiliary heat exchanger is obtained. The capacity of this element, the mass flux and the outlet temperature of the secondary fluid are calculated from the following equations:

$$\dot{Q}_{aux} = \dot{m}_3(h_{203} - h_{202}) \tag{2.22}$$

$$\dot{Q}_{aux} = \dot{m}_{aux} c_{p,aux}(T_{aux,i} - T_{aux,o}) \tag{2.23}$$

$$\dot{Q}_{aux} = U_{o,aux} F_{aux} A_{o,aux} \Delta T_{lm,aux} \tag{2.24}$$

At the outlet of this heat exchanger, the super-heating (h_{203}) needed to evaporate the refrigerant and to drag the oil to the compressor is fixed. The global heat transfer coefficient, $U_{o,aux}$, the flow configuration factor, F_{aux}, and the refrigerant pressure loss in the auxiliary heat exchanger are evaluated from manufacturer's data, as in the case of the condenser. The inlet temperature $T_{aux,i}$ of the secondary fluid is known as a boundary condition. In the node where points 12 and 204 connect with point 13, another energy balance is made in order to evaluate h_{13}.

2.2.4 Algorithm of resolution

Beginning with an initial value of the suction and discharge pressure of the compressor, all the enthalpies and pressures are computed for each element, iterating until convergence is reached. Variables like velocities are also calculated to ensure that the designed tube dimensions are correct. Figure 2.3 shows the resolution sequence of the different elements of the liquid overfeed system.

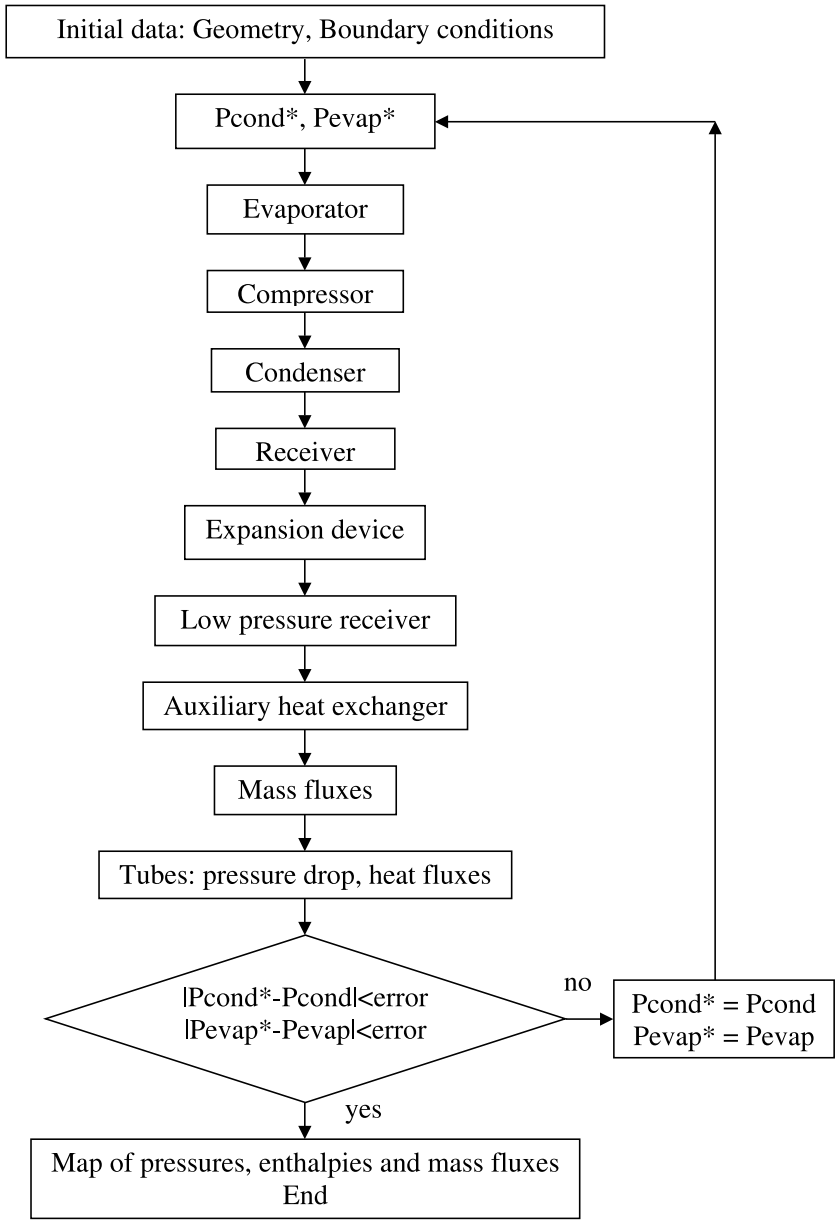

Figure 2.3: Numerical resolution of the liquid overfeed refrigeration system

2.3 Compact heat exchanger simulation model

Compact heat exchangers (fin-and-tube) are used where gas-liquid heat transfer is necessary, and are employed in many industries and applications. Some examples are the refrigeration and air conditioning industries (evaporators and condensers), the automobile industry (radiators), as dehumidifying exchangers, for heat recovery from combustion, etc.

Even though compact heat exchangers are widely used in industry for years, optimal designs are very difficult to obtain due to the extremely complex geometrical configurations and physical phenomena involved. The analytical methods, often used for heat exchanger design (F-factor,ε-NTU), are restricted by a large number of hypothesis (steady state, uniform heat transfer coefficient, constant thermo-physical properties, etc). On the other hand, computational simulations, based on the discretization of the heat exchanger into control volumes for which the governing equations (mass, momentum and energy) are solved, permit to overcome the majority of limitations existing with the analytical methods.

A mathematical model of compact heat exchangers has been specially developed in the CTTC for the detailed fluid-dynamic simulation of these equipment. The model has been consolidated under the name CHESS (Compact Heat Exchanger Simulation Softwear), and presented in various publications, [2], [3]. The simulation deals with evaporators and condensers for air conditioning and refrigeration, and with heat exchangers using liquid refrigerants, as automotive radiators, air-coolers and heaters.

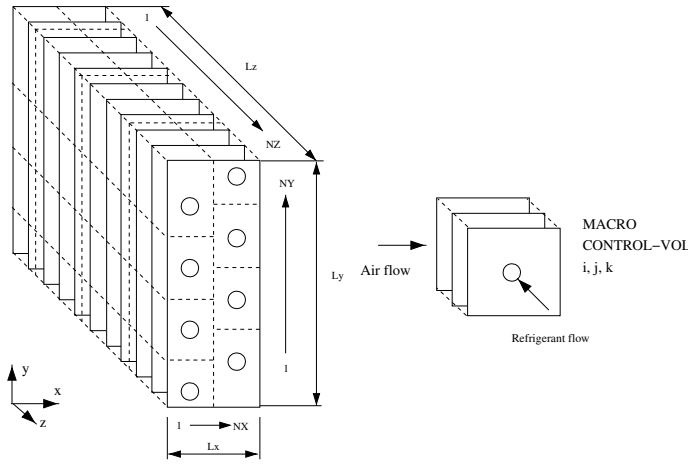

Figure 2.4: Macro control volumes discretization

Expanded, galvanized and brazed fin-and-tube compact heat exchanger geometries are implemented.
The physical phenomena produced in compact heat exchangers are very complex, unsteady, three-dimensional, and usually with turbulent flow regimes. Wide variety of geometries are available, with different relative positions of the tubes, numerous fin shapes and circuitry arrangement possibilities. In order to approach the problem under these conditions, the model adopts a strategy of resolution based on discretization of the heat exchanger into macro control volumes around the tubes, Figure 2.4. Over these macro control volumes the equations of conservation of mass, momentum and energy are applied for both fluids, and the energy equation for the solid elements. The fluid-solid interaction is represented with friction factors, heat transfer coefficients and local pressure loss coefficients, obtained from basic experimental correlations published in the open literature.

2.3.1 Internal flow analysis

The internal flow is resolved integrating the governing equations (mass, momentum and energy) over the interior of the tube section corresponding to the macro control volume of the heat exchanger. The formulation is developed in general form considering two-phase fluid, according [13], [14], [15]. The single-phase flow of liquid or vapour can be analysed with the same mathematical formulation as particular cases of two-phase flow. The equations of mass, momentum and energy, integrated over a finite control volume, assuming one dimensional flow and neglecting axial heat conduction, are written in the following form:

$$0 = \dot{m}_o - \dot{m}_i + \frac{\partial m}{\partial t} \tag{2.25}$$

$$\begin{aligned}(p_i - p_o)S - \tilde{\tau}P\Delta z - mgsin\theta = \dot{m}_{g,o}v_{g,o} - \dot{m}_{g,i}v_{g,i} + \\ \dot{m}_{l,o}v_{l,o} - \dot{m}_{l,i}v_{l,i} + \Delta z\frac{\partial \tilde{\dot{m}}}{\partial t}\end{aligned} \tag{2.26}$$

$$\begin{aligned}\tilde{q}P\Delta z = \dot{m}_{g,o}(e_{g,o} - e_{l,o}) - \dot{m}_{g,i}(e_{g,i} - e_{l,i}) + \bar{\dot{m}}(e_{l,o} - e_{l,i}) + \\ (\tilde{e}_g - \tilde{e}_l)\frac{\partial m_g}{\partial t} + m_g\frac{\partial \tilde{e}_g}{\partial t} + m_l\frac{\partial \tilde{e}_l}{\partial t} - S\Delta z\frac{\partial \tilde{p}}{\partial t} + (\tilde{e}_l - \bar{e}_l)\frac{\partial m}{\partial t}\end{aligned} \tag{2.27}$$

The specific energy is denominated in equation (2.27) with $e = h + v^2/2 + gz\sin\theta$. The symbols "$\tilde{}$" and "$\bar{}$" indicate respectively the integral mean over the control volume and the arithmetical mean between inlet and outlet of the control volume. The term $(\tilde{e}_l - \bar{e}_l)\frac{\partial m}{\partial t}$ is zero for differential control volume and negligible for a finite discretization control volume. For the convection heat transfer the superficial coefficient of convective heat transfer α has been introduced with the equation: $\dot{q} = \alpha(T_w - T_f)$,

where T_w is the wall temperature.
The mathematical model requires empirical information about the friction factor f, the pressure loss in singularities (contractions, expansions, bends), the coefficient of convective heat transfer α and the void fraction ε_g. This information is generally obtained from empirical and semi-empirical correlations.
In the zones of flow without phase change the convective coefficient of heat transfer is calculated using the equations of Nusselt and Gnielinski [10] for laminar and turbulent flow respectively. The friction factor is calculated from Churchill's equation [7].
In two-phase flow variety of correlations can be applied depending on the flow regime. Correlations based on the two-phase flow pattern are also available. Detailed description of the different empirical correlations used in the simulation is given in [15], together with studies and comparisons between them.
The internal flow configurations in compact heat exchangers are very diverse, often with flow divisions in different circuits, and merging in common collectors. The flow distribution across the heat exchanger is determined by fixing a uniform outlet pressure for all the circuits. The flow passing through each circuit is determined in function of the flow resistance using an iterative calculation scheme.

2.3.2 Air-flow analysis

The code calculates the heat transfer and pressure loss at each macro control volume by the resolution of the adequate mass, momentum and energy balances, equations (2.28) to (2.30), according [2], assuming a uniform velocity distribution across the flow section (unidimensional treatment). The global air-flow is distributed depending on the resistance of each zone of the heat exchanger, to get a uniform outlet pressure.

$$0 = \dot{m}_o - \dot{m}_i + \frac{\partial m}{\partial t} \tag{2.28}$$

$$(p_i - p_o)S - \tilde{\tau} A_a = \dot{m}_o v_o - \dot{m}_i v_i + \frac{\partial \tilde{\dot{m}}}{\partial t}\frac{V}{S} \tag{2.29}$$

$$\alpha_a (T_w - \bar{T}_a)\eta'_a A_a = \dot{m}_o e_o - \dot{m}_i e_i + \frac{\partial(\rho\tilde{e})}{\partial t}V - \frac{\partial p}{\partial t}V \tag{2.30}$$

The developed mathematical model needs the evaluation of heat transfer coefficients and friction factors. Currently, the code uses basic experimental correlations published in the literature, [16], [17], [18].
Related to heat transfer, a local calculation of the dew-point temperature permits a determination of the dry and wet zones on the air-side surfaces, and consequently of the sensible/latent heat ratios and vapour condensation rates at each macro control volume. This is of great importance in compact evaporators and air-coolers. If wet

conditions are present, with surface temperature below the freezing point, frost formation is analysed, calculating the changes in frost thickness and frost density. Thus, a dry heat exchanger becomes a particular case of this analysis.
The moist air-flow mathematical formulation is presented in detail in reference [3].
As refers to the air fluid-dynamic behaviour of the heat exchanger, the code predicts the inlet/outlet pressure drop effects and the changes in kinetic energy, in steady and unsteady analysis.

2.3.3 Solid elements analysis

The thermal analysis of the solid elements is based on the resolution of the multidimensional conduction heat transfer equation. Heat conduction along the tubes is considered, together with a detailed analysis of the fin efficiency and the tube thermal contact resistance. The tubes are analysed applying energy balance in each macro control volume, including the heat transfer to the refrigerant, the heat transfer to the air, the accumulated heat, and the heat conduction between the adjacent solid volumes. A set of materials is introduced (copper, steel, galvanized steel, aluminium, brass) with variable physical properties.
Continuous fin geometry is commonly used in expanded tube and galvanized heat exchangers, of wide use in refrigeration and air conditioning, but also in some low-power automotive radiators. For the simulation of the fins two different approaches can be used, [3].
In the basicCHESS model the fin efficiency is evaluated as that of a circular fin with adiabatic boundary, neglecting at this manner the heat conducted through the fins between the adjacent tubes.
In the advancedCHESS model a multidimensional simulation of the fin is performed and the longitudinal and transversal conduction heat transfer is calculated. One fin for each level of axial discretization of the heat exchanger is simulated. The code integrates for the zones corresponding to the macro control volume the heat fluxes tube-fin and fin-air, and the water condensate fluxes obtained with the multidimensional fin simulation, and calculates real fin efficiency for each macro control volume. This model has an advantage where the fin conductivity is directionally dependent. In these cases the hypothesis of adiabatic boundary condition for the calculation of the fin efficiency used in the basic model might not be adequate. The computational cost expressed in terms of calculation time is greater than for the basic model.

2.3.4 Numerical simulation

The numerical resolution of the internal fluid flow is coupled with the resolution of the air-flow and the heat conduction in the solid elements in a segregated way within a global fully implicit transient resolution algorithm.

The internal flow resolution of the governing equations is carried out over the macro control volumes using step-by-step method in the direction of flow. From the known values of the variables at the inlet section, considering the temperature distribution in the tube walls as a boundary condition, the variables at the outlet of the control volume are obtained. This solution is used as an inlet condition for the next control volume. Convergence criterion must be verified in each control volume for passing to the next one.
For the air-flow the governing equations are resolved considering uniform air distribution over each macro control volume cross-section. The global air-flow is divided depending on the flow resistance in each heat exchanger zone, in order to obtain the same outlet pressure. The inlet/outlet effects are considered, as well as the internal acceleration of the air due to temperature change. A local calculation of the psychrometrical dew-point permits the determination of the dry and wet zones on the air-side surface, and consecutively the sensible-latent heat ratio and the condensed water quantity in each macro control volume. If condensation conditions exist and the surface temperature is below freezing point, to analysis of frost formation is proceeded, calculating the frost width changes and density, according to [2] and [15].
The solid elements (tubes, elbows, collectors) are analysed applying energy balances in each macro control volume, considering the heat transfer with the air, the internal flow, the conduction to adjacent control volumes, and the heat accumulation term.
In heat exchangers with continuous fin geometry, two different approaches of simulation can be used. The basic model evaluates the fin efficiency as that of a circular fin with adiabatic boundary. In cases where neighbour tube temperatures are considerably different, the adiabatic boundary condition for the evaluation of the fin efficiency is no longer adequate. In these cases the code uses a multidimensional simulation of the continuous fins from which real fin efficiency is calculated for each macro control volume.
The resolution of the internal flow, the air-flow and the solid elements is carried out iteratively until the adopted convergence criterion, based in the desired precision for each magnitude, is verified.

2.4 Conclusions

In this chapter the numerical models to which the developed experimental infrastructures are oriented, have been presented. A model of liquid overfeed refrigeration system is presented, capable to predict the operation of the system in steady state regime. The system model is based on the sequential resolution of the different components of the system, for which simplified mathematical models are used. The components are modelized on the basis of parameters from higher level simulations (evaporator), manufacturer data (compressor, condenser), and global balances of mass, momentum

and energy. Under the defined component characteristics, geometry and boundary conditions, the model predicts the operating point of the system, calculating temperatures, pressures and flow-rates throughout the system, as well as the evaporator and condenser capacities. The refrigerant velocities, the pressure losses, and the heat transfer in the connecting tubes are calculated, giving to the model features, permitting it to be used as a design assisting tool.

An existing numerical compact heat exchanger simulation model (CHESS) has been presented. The model adopts a strategy of resolution based on discretization of the heat exchanger into macro control volumes around the tubes, over which the governing equations are resolved. The model uses variable thermo-physical properties, and only basic empirical information about the heat transfer coefficients and the friction factors. It deals with evaporators, condensers and compact heat exchangers using liquid refrigerants. Different geometries, as expanded, galvanized and brazed fin-and-tube compact heat exchangers, have been implemented.

The above commented numerical models have been used extensively to assist the design of the experimental infrastructure, especially in determining the working range, components selection, dimensioning and prototype selection.

2.5 Nomenclature

A	heat transfer area $[m^2]$
A_o	global heat transfer area $[m^2]$
c_p	specific heat capacity at constant pressure $[J/kgK]$
D	diameter $[m]$
e	specific energy $[J/kg]$
f	friction factor
F	configuration factor
g	gravity $[m/s^2]$
h	enthalpy $[J/kg]$
k	local loss coefficient
m	mass $[kg]$
M	oil concentration [kg oil/kg ref]
$\dot{m}$	mass flow rate $[kg/s]$
p	pressure $[Pa]$
P	perimeter $[m]$
$\dot{q}$	heat flux per unit surface $[W/m^2]$
$\dot{Q}$	heat flux $[W]$
S	transversal area $[m^2]$
t	time $[s]$
T	temperature $[K]$
U	heat transfer coefficient$[W/m^2K]$
U_o	global heat transfer coefficient of heat exchanger$[W/m^2K]$
v	velocity $[m/s]$
V	volume $[m^3]$
x_g	vapour quality

Greek symbols

α	convective heat transfer coefficient $[W/m^2K]$
Δp	pressure drop $[Pa]$
Δt	time step $[s]$
Δz	control volume length or height difference $[m]$
ε_g	volumetric fraction of vapour or void fraction
η	efficiency
η'	global fin efficiency (fin-and-tube)
λ	thermal conductivity $[W/mK]$
ρ	density $[kg/m_3]$
τ	shear stress $[N/m_2]$
θ	inclination angle

Subscripts

aux	auxiliary
cd	condenser
cp	compressor
e	evaporator
E	electrical
em	electrical-mechanical
ext	external
f	fluid
fr	friction
g	gas or vapour
i	inlet or inner
in	inlet
ins	insulation
l	liquid
lm	logarithmic mean
loc	local
lpr	low-pressure receiver
o	outlet or outer
out	outlet
p	pump
s	secondary fluid
si	secondary inlet
so	secondary outlet
sat	saturated
sep	oil separator
$tube$	tube
w	wall, water

References

[1] García-Valladares O., Pérez-Segarra C.D., Oliet C., and Danov S. Numerical Studies of Refrigerating Liquid Overfeed Systems Working with Ammonia and R134a. In *International Refrigeration and Air Conditioning Conference at Purdue*, volume 1, pages 327–334, 2000.

[2] Oliet C., Pérez-Segarra C.D., García-Valladares O., and Oliva A. Advanced Numerical Simulation of Compact Heat Exchangers. Application to Automative, Refrigeration and Air-Conditioning Industries. In *Proceedings of the European Congress on ComputationalMethods in Applied Sciences and Engineering (ECCOMAS)*, Barcelona, 2000.

[3] Oliet C., Pérez-Segarra C.D., Danov S., and Oliva A. Numerical Simulation of Dehumidifying Fin-and-tube Heat Exchangers. Model Strategies and Experimental Comparisons. In *Ninth International Refrigeration and Air Conditioning Conference at Purdue*, 2002.

[4] *Refrigeration Handbook*. ASHRAE, 1998.

[5] Wilbert F. Stoecker. *Industrial Refrigeration Handbook*. McGraw-Hill, 1998.

[6] National Institute of Standards and Technology. *NIST Thermodynamic and Transport Properties of Refrigerants and Refrigerant Mixtures - REFPROP v6.01.*, Gaithersburg, MD, USA, 1998.

[7] Churchill S. W. Frictional equation spans all fluid flow regimes. *Chemical Engineering*, 84:91–92, 1977.

[8] Lockhart R. W. and Martinelli R. C. Proposed correlation of data for isothermal two-phase, two-component flow in pipes. *Chemical Engineering Progress*, 45(1):39–48, 1949.

[9] Friedel L. Improved friction pressure drop correlation for horizontal and vertical two-phase pipe flow. In *European Two-Phase Flow Group Meeting, Ispra, Italy, Paper E2*, 1979.

[10] Gnielinski V. New equations for heat and mass transfer in turbulent pipe and channel flow. *International Chem. Eng.*, 16:359–368, 1976.

[11] Shah M. M. Chart correlation for saturated boiling heat transfer: Equations and further study. *ASHRAE Transactions*, 88:185–196, 1982.

[12] Viktor L. Streeter, E. Benjamin Wylie, and Keith W. Bedford. *Fluid Mechanics*. McGraw-Hill, 9th edition, December 1997.

[13] Escanes F., Pérez-Segarra C. D., and Oliva A. Thermal and fluid-dynamic behaviour of double-pipe condensers and evaporators. *International Journal of Numerical Methods for Heat and Fluid Flow*, vol.5(no.9):pp.781–795, 1995.

[14] García-Valladares O., Pérez-Segarra C.D., Rigola J., and Oliva A. Detailed numerical simulation of condensers and evaporators using pure and mixed refrigerant. In *International Compressor Engineering Conference at Purdue*, volume 2, pages 839–844, 1998.

[15] Octavio García Valladares. *Simulación numérica y validación experimental de evaporadores, condensadores y tubos capilares. Integración en sistemas de refrigeración por compresión.* PhD thesis, Universitat Politècnica de Catalunya, 2000.

[16] A. Achaichia and T.A. Cowell. Heat transfer and pressure drop characteristics of flat tube and louvered plate fin surfaces. *Experimental Thermal and Fluid Science*, vol.1:pp.147–157, 1988.

[17] Y. Chang and C. Wang. A generalized heat transfer correlation for louver fin geometry. *Int. Journal of Heat and Mass Transfer*, vol.40(no.3):pp.533–544, 1997.

[18] C.J. Davenport. Correlations for heat transfer and flow friction characteristics of louvered fin. *AIChE Symposium Series*, vol.79(no.225):pp.19–27, 1983.